AEM
Journals.ASM.org

Comparative Transcriptomic Analysis of the *Burkholderia cepacia* Tyrosine Kinase *bceF* Mutant Reveals a Role in Tolerance to Stress, Biofilm Formation, and Virulence

Ana S. Ferreira,[b] Inês N. Silva,[b] Vítor H. Oliveira,[b] Jörg D. Becker,[c] Michael Givskov,[d] Robert P. Ryan,[e] Fábio Fernandes,[f] Leonilde M. Moreira[a,b]

Department of Bioengineering, Instituto Superior Técnico, Lisbon, Portugal[a]; Institute for Biotechnology and Bioengineering, Centre for Biological and Chemical Engineering, Instituto Superior Técnico, Lisbon, Portugal[b]; Instituto Gulbenkian de Ciência, Oeiras, Portugal[c]; Department of International Health, Immunology and Microbiology, University of Copenhagen, Copenhagen, Denmark, and Singapore Centre on Environmental Life Sciences Engineering, Nanyang Technological University, Singapore[d]; Division of Molecular Microbiology, College of Life Sciences, University of Dundee, Dundee, United Kingdom[e]; Centro de Química Física Molecular and Institute of Nanosciences and Nanotechnologies, Instituto Superior Técnico, Lisbon, Portugal[f]

The bacterial tyrosine-kinase (BY-kinase) family comprises the major group of bacterial enzymes endowed with tyrosine kinase activity. We previously showed that the BceF protein from *Burkholderia cepacia* IST408 belongs to this BY-kinase family and is involved in the biosynthesis of the exopolysaccharide cepacian. However, little is known about the extent of regulation of this protein kinase activity. In order to examine this regulation, we performed a comparative transcriptome profile between the *bceF* mutant and wild-type *B. cepacia* IST408. The analyses led to identification of 630 genes whose expression was significantly changed. Genes with decreased expression in the *bceF* mutant were related to stress response, motility, cell adhesion, and carbon and energy metabolism. Genes with increased expression were related to intracellular signaling and lipid metabolism. Mutation of *bceF* led to reduced survival under heat shock and UV light exposure, reduced swimming motility, and alteration in biofilm architecture when grown *in vitro*. Consistent with some of these phenotypes, the *bceF* mutant demonstrated elevated levels of cyclic-di-GMP. Furthermore, BceF contributed to the virulence of *B. cepacia* for larvae of the Greater wax moth, *Galleria mellonella*. Taken together, BceF appears to play a considerable role in many cellular processes, including biofilm formation and virulence. As homologues of BceF occur in a number of pathogenic and plant-associated *Burkholderia* strains, the modulation of bacterial behavior through tyrosine kinase activity is most likely a widely occurring phenomenon.

Bacterial tyrosine kinases (BY-kinases) are best characterized for regulating the biosynthesis and the export of bacterial extracellular carbohydrate polymers in both Gram-positive and Gram-negative bacteria. These proteins comprise two domains: a transmembrane activator domain with a large extracellular loop and an intracellular catalytic domain encompassing the ATP-binding site and tyrosine-rich region (1). These two domains can either be linked in a single polypeptide, such as in *Proteobacteria* and *Actinobacteria*, or split into two separate proteins encoded by adjacent genes, as in the *Firmicutes* (1). Resolution of the BY-kinase tridimensional structures showed no resemblance to their mammalian counterparts, and therefore these proteins are seen as good targets for antibacterial drug design (2).

A number of studies have shown the importance of BY-kinases in polysaccharide biosynthesis, mainly as components of a multienzymatic complex responsible for polysaccharide polymerization and export (3). Moreover, several enzymes involved in sugar-nucleotide biosynthesis and repeat unit formation have also been identified as phosphorylation targets of BY-kinases. For example, *Escherichia coli* Wzc and *Bacillus subtilis* PtkA BY-kinases were found to phosphorylate UDP-glucose dehydrogenase enzymes (4, 5), EpsD from *Streptococcus thermophilus* (6) and Wzc of *Klebsiella pneumoniae* (7) were found to phosphorylate the undecaprenyl-phosphate glycosyltransferases EpsE and WcaJ, respectively, and Cap5B2 from *Staphylococcus aureus* was found to phosphorylate the UDP-acetyl-mannosamine dehydrogenase Cap5O (8). In addition, BY-kinases have been demonstrated to have other cellular targets not related to polysaccharide biosynthesis, as is the case for the *E. coli* alternative heat shock sigma factor RpoH and the RpoE anti-sigma factor RseA (9), integrase proteins (Int) of coliphage HK022 (10), and single-stranded DNA-binding proteins SsbA and SsbB from *Bacillus subtilis* (11). Besides the genetic and biochemical analyses of individual targets of BY-kinases reported above, other bacterial tyrosine-phosphorylated proteins have been identified by gel-free proteomics approaches in organisms such as *E. coli* (12), *B. subtilis* (13, 14), *Listeria monocytogenes* (15), *Streptococcus pneumoniae* (16), and *Pseudomonas* species (17), to name a few. These tyrosine-phosphorylated proteins are involved in several cellular processes, such as stress responses, DNA metabolism, transcription, translation, central metabolism, cell division, and cell wall polysaccharide biosynthesis, among others (18, 19). A recent study demonstrated that tyrosine phosphorylation on target proteins not only modulates their enzymatic activity but also their correct cellular localization (20), adding a new dimension to the role of tyrosine phosphorylation in the bacterial cell.

Bacteria belonging to *Burkholderia cepacia* complex (Bcc) are

Received 28 January 2013 **Accepted** 20 February 2013
Published ahead of print 22 February 2013
Address correspondence to Leonilde M. Moreira, lmoreira@ist.utl.pt.
Supplemental material for this article may be found at http://dx.doi.org/10.1128/AEM.00222-13

doi:10.1128/AEM.00222-13

TABLE 1 Strains and plasmids used in this study

Strain or plasmid	Genotype or description[a]	Reference or source
Escherichia coli strains		
XL1-Blue	*recA1 lac* [F′ *proAB lacI*^{q} *Z*αM15 Tn*10* (Tc^{r})] *thi*	51
αDH5	*recA1* Δ*lacU169* ϕ80 *lacZ*ΔM15	BRL
Burkholderia cepacia strains		
IST408	Cystic fibrosis isolate, EPS^{+}	22
IST408 *bceE*::Tp	IST408 derivative with *bceE* gene disrupted by Tp^{r} gene cassette	This work
IST408 *bceF*::Tp	IST408 derivative with *bceF* gene disrupted by Tp^{r} gene cassette	28
Plasmids		
pBCSK	Phagemid derived from pUC19, Cm^{r}	Stratagene
pRK2013	Tra^{+} Mob^{+} (RK2) Km::Tn*7* ColEl origin, helper plasmid, Km^{r}	52
pUC-TP	pUC-GM derivative with 1.1-kb Tp^{r} gene cassette, Ap^{r} Tp^{r}	53
pDA17	*ori*$_{pBBR1}$ P$_{DHFR}$ Tet^{r}	54
pIN25	*ori*$_{pBBR}$ Δ*mob*, GFP, Cm^{r}	55
pLM56-1	pBCSK derivative containing 2,411-bp KpnI/EcoRI fragment encompassing *bceE* and flanking regions	This work
pLM56-4	pLM56-1 derivative containing Tp^{r} gene cassette at XhoI site disrupting *bceE*	This work
pLM127-4	pDA17 derivative containing 1,329-bp NdeI/XbaI fragment with *rpoH* coding region	This work
pLM127-9	pDA17 derivative containing 2,239-bp NdeI/XbaI fragment with *bceF* coding region	This work
pLM127-11	pDA17 derivative containing 1,100-bp NdeI/XbaI fragment with *bceE* coding region	This work

[a] Abbreviations: Cm^{r}, chloramphenicol resistance; Tp^{r}, trimethoprim resistance; Ap^{r}, ampicillin resistance; Tet^{r}, tetracycline resistance; Km^{r}, kanamycin resistance.

important opportunistic pathogens, especially for cystic fibrosis (CF) and chronic granulomatous disease patients. These pathogens can cause deterioration of lung function, and some patients develop a condition known as cepacia syndrome, characterized by a fatal necrotizing pneumonia accompanied by septicemia (21). Bcc bacteria produce a variety of virulence factors, one of them being the exopolysaccharide (EPS) cepacian produced by most Bcc isolates (22–24). This EPS is thought to be involved in persistence of the bacteria in CF lungs by their interactions with antimicrobial peptides, by interfering with the function of key components of the pulmonary host defense due to their capacity to scavenge reactive oxygen species, and by their involvement in biofilm formation (reviewed in reference 25). Another exopolysaccharide of *Burkholderia* was recently identified as relevant for biofilm matrix formation (26). The chemical structure of this new EPS has not yet been determined, but its biosynthetic genetic locus (gene cluster BCAM1330-BCAM1341 in *Burkholderia cenocepacia* J2315) encompasses several typical EPS-related genes encoding putative glycosyltransferases, polysaccharide-modifying enzymes, polysaccharide export proteins, and a BY-kinase protein (26). Among the genes involved in the biosynthesis of the exopolysaccharide cepacian is *bceF*, which encodes another BY-kinase (27). Disruption of the *bceF* gene compromised cepacian biosynthesis and the ability to produce thick biofilms *in vitro* (28). Furthermore, mortality was completely absent in gp91$^{phox-/-}$ mice challenged with a *bceF* transposon mutant, while in another mutant for the *bceI* gene, which encodes a putative polysaccharide polymerase, infected mice died 5 days later than those infected with the wild-type *Burkholderia cepacia* IST408 strain (29). The differences in virulence of the *bceF* and *bceI* EPS-deficient transposon mutants (29), together with the knowledge that BY-kinases have several endogenous targets in the cell, prompted us to evaluate which cellular processes require the BceF tyrosine kinase and may account for the observed differences in virulence. To accomplish this, transcriptome profiling of the wild-type *B. cepacia* IST408 and the EPS-deficient *bceF*::Tp and *bceE*::Tp isogenic insertion mutants was carried out. Based on the gene expression results, a series of phenotypic traits were compared to identify the pathways in which this BY-kinase may play a role.

MATERIALS AND METHODS

Bacterial strains, plasmids, and growth conditions. The strains and plasmids used in this work are listed in Table 1. *E. coli* was grown in LB medium at 37°C. Unless otherwise stated, *B. cepacia* strains were grown in LB, pseudomonas isolation agar (PIA), or in EPS-producing S medium at 30°C (22). Growth media were supplemented with antibiotics when required to maintain the selective pressure at the following concentrations (in μg/ml): for *B. cepacia*, trimethoprim at 100, chloramphenicol at 300, and tetracycline at 400; for *E. coli*, trimethoprim at 100, chloramphenicol at 25, ampicillin at 100, tetracycline at 10, and kanamycin at 50.

DNA manipulation techniques. Total DNA was extracted from bacterial cells by using the DNeasy blood and tissue kit (Qiagen), following the manufacturer's instructions. Plasmid DNA isolation and purification, DNA restriction/modification, agarose gel electrophoresis, and *E. coli* transformation were carried out using standard procedures (30). *B. cepacia* electrocompetent cells, prepared as previously described (28), were transformed by electroporation using a Bio-Rad Gene Pulser II (200 Ω, 25 μF, 2.5 kV) and grown overnight before being plated in selective medium. Plasmids for complementation experiments and pIN25 expressing the green fluorescence protein (GFP) were mobilized into *Burkholderia cepacia* strains by triparental conjugation using plasmid pRK2013 as the helper.

Construction of the *bceE* insertion mutation. To obtain a *B. cepacia* IST408 *bceE* disruption, a 2,411-bp KpnI/EcoRI fragment containing the *bceE* coding region and flanking regions was amplified using primers BceE-up (5′-CGA*GGTACC*CGTGATCGTCA; restriction sites are shown in italics) and BceE-low (5′-GAT*GAATTC*GACGTCGGCCACTT) and cloned into the same restriction sites of pBCSK. The plasmid obtained (pLM56-1) was further digested with XhoI, which has a single recognition site within the *bceE* coding region. The trimethoprim (Tp) resistance cas-

sette was obtained from pUC-TP and was cloned into pLM56-1, resulting in the plasmid pLM56-4, which transcribed the cassette in the same orientation as the *bceE* gene. This plasmid was introduced into *B. cepacia* IST408 by electroporation, and transformants were selected by growth on PIA medium with trimethoprim. The colonies obtained were then screened in the presence of chloramphenicol. Colonies that did not grow in the presence of chloramphenicol but were trimethoprim resistant were considered candidates for allelic exchange of *bceE* by the *bceE*::Tp construct. The candidate insertion mutant was further characterized by PCR amplification and DNA sequencing.

Construction of plasmids for complementation experiments. PCR was used to amplify the coding region of *bceE* (primers bceE-fw, 5′-GAA*CATATG*CTGAAACGCCCGATG, and bceE-rev, 5′-TGA*TCTAGA*GGAGCAGCTGGCCGAGGA; restriction sites are in italics); *bceF* (primers bceF-fw, 5′-GAA*CATATG*GTGAACACGCAAGCGAAA, and bceF-rev, 5′-TTA*TCTAGA*ATGCGGATCAGGCGCTCA), and *rpoH* (BCAL0787 in *B. cenocepacia* J2315; primers rpoH-fw, 5′-TTT*CATATG*AGCAACGCCCTGACCCTC, and rpoH-rev, 5′-CCG*TCTAGA*AACCGGTGGAAAAAATTG). Following restriction with NdeI and XbaI, each gene was cloned in the same restriction sites of pDA17. The plasmids obtained were pLM127-4, pLM127-9, and pLM127-11, carrying the *rpoH*, *bceF*, and *bceE* genes, respectively (Table 1). The nucleotide sequences of the cloned genes were confirmed by DNA sequencing.

Isolation and processing of RNA and DNA samples. For expression profiling, overnight cultures of wild-type *B. cepacia* IST408 and the isogenic mutants *bceE*::Tp and *bceF*::Tp were grown in LB medium and diluted into S medium to an initial optical density at 640 nm (OD_{640}) of 0.1. Triplicate 250-ml Erlenmeyer flasks containing 100 ml of medium were inoculated with each strain and cultured at 30°C with agitation at 250 rpm for 12 h. These bacterial cells were resuspended in RNAprotect bacteria reagent (Qiagen), and total RNA extraction was carried out using the RNeasy minikit (Qiagen), followed by DNase treatment (RNase-free DNase set; Qiagen) according to the manufacturer's recommendations. RNA integrity was checked on an Agilent 2100 Bioanalyser using an RNA Nano assay. RNA was processed for use on Affymetrix custom dual-species *Burkholderia* arrays (31), according to the manufacturer's prokaryotic target preparation assay instructions. Briefly, 10 μg of total RNA containing spiked poly(A) RNA controls [GeneChip poly(A) RNA control kit; Affymetrix, Santa Clara, CA] was used in a reverse transcription reaction with random primers (Invitrogen Life Technologies) to generate first-strand cDNA. After removal of RNA, 2 μg of cDNA was fragmented with DNase and end labeled with biotin by using terminal polynucleotidyl transferase (GeneChip WT terminal labeling kit; Affymetrix). The size distribution of the fragmented and end-labeled cDNA was assessed using the Agilent 2100 Bioanalyzer. Two micrograms of end-labeled fragmented cDNA was used in a 200-μl hybridization cocktail containing hybridization controls, and the mixture was hybridized on arrays for 16 h at 50°C. Modified posthybridization wash and double-stain protocols (FLEX450_0005; GeneChip HWS kit; Affymetrix) were used on a GeneChip fluidics station 450. Arrays were scanned on an Affymetrix GeneChip scanner 3000 7G. Biological triplicates of RNA from each bacterial culture were processed and analyzed.

For DNA analysis, a total of 1.5 μg of genomic DNA from *B. cepacia* IST408 was labeled using the Bioprime DNA labeling system (Invitrogen, Paisley, United Kingdom) following a strategy for genomic DNA hybridization to GeneChips developed by Hammond and coauthors (32). Cleanup was performed using the MinElute PCR purification kit (Qiagen, Hilden, Germany), and quality was checked on an Agilent 2100 Bioanalyser using a DNA 1000 assay. Five micrograms of labeled DNA was analyzed on an Affymetrix custom dual-species *Burkholderia* array following the protocol described above for RNA samples.

Microarray analysis. For microarray analysis, DNA-based probe selection was performed using Xspecies DNA hyb CDF batchmaker v3.2 (32; http://affymetrix.arabidopsis.info/xspecies/). An optimal signal cutoff of 80 and minimum number of probes per probe set of 7 were determined empirically, resulting in the masking of 24,223 of the original 226,576 probes on the array and the exclusion of 156 probe sets. The new cdf file created (Bcc1sa520656F_Xspecies.CEL80.cdf) was used in a DNA Chip Analyzer 2008 for the subsequent gene expression analyses. The 9 expression arrays were normalized to a baseline array with median CEL intensity by applying an invariant set normalization method (33). Normalized CEL intensities of the arrays were used to obtain model-based gene expression indices based on a perfect match (PM)-only model (34). Replicate data (triplicates) for each bacterial isolate were weighted gene-wise by using the inverse squared standard errors as weights. All genes compared were considered differentially expressed if the 90% lower confidence bound of the fold change (LCB) between the experimental value and baseline was above 1.2. The lower confidence bound criterion meant that we could be 90% confident that the fold change was a value between the lower confidence bound and a variable upper confidence bound. Li and Wong have shown that the lower confidence bound is a conservative estimate of the fold change and therefore more reliable as a ranking statistic for changes in gene expression (33).

This comparison resulted in 630 differentially expressed transcripts with a median false-discovery rate (FDR) of 1.7% when the *bceF*::Tp mutant was compared with the wild-type IST408. The comparison of the *bceE*::Tp mutant transcriptome with the one of IST408 showed 5 genes differentially expressed (≥1.6-fold change lower confidence bound, with a resulting FDR of 0%).

qRT-PCR assays. DNA microarray data were validated by real-time quantitative reverse transcription-PCR (qRT-PCR) as previously described (24). Total RNA was used in a reverse transcription reaction with TaqMan reverse transcription reagents (Applied Biosystems). qRT-PCR amplification of each gene (for primer sequences, see Table S1 in the supplemental material) was performed with a model 7500 thermocycler (Applied Biosystems). The expression ratio of the target genes was determined relative to the reference gene *lepA*, which showed no variation in transcript abundance under the conditions tested. Relative quantification of gene expression by real-time qRT-PCR was determined using the $\Delta\Delta C_T$ method (35).

***In vivo* complementation of EPS-deficient strains.** Plasmids pDA17, pLM127-9 (+p*bceF*), and pLM127-11 (+p*bceE*) were mobilized into the parental strains IST408, IST408 *bceF*::Tp, and IST408 *bceE*::Tp, respectively, by triparental conjugation. To determine their ability to restore cepacian biosynthesis *in vivo* these strains were grown in liquid S medium over 3 days at 30°C. EPS quantification was based on the dry weight of EPS recovered after ethanol precipitation of culture supernatants, as described before (28).

Stress conditions. Survival of *Burkholderia* strains to heat stress was tested by inoculation of overnight cultures into 4 ml of S medium to a final OD_{640} of 0.1. Strains were allowed to grow until the OD_{640} reached 0.6 before being submitted to a static incubation at 50°C in a water bath for 20 min. At 4- or 8-min intervals, an aliquot of 100 μl was serially diluted and plated onto LB agar. After 48 h of incubation at 30°C, CFU were counted. To test tolerance to UV irradiation, 500-μl aliquots of the bacterial cell suspensions prepared in S medium (OD_{640}, 0.1) were transferred into PMMA cuvettes (VWR) and immediately exposed to UV irradiation (λ, 254 nm) for different times. Aliquots from each cell suspension were serially diluted and plated onto LB agar, and plates were incubated for 2 days at 30°C before CFU counting. Each experiment was repeated at least three times.

Detection of cyclic-di-GMP. The method for detection of cyclic-di-GMP from *B. cepacia* IST404 and its derivative mutants *bceF*::Tp and *bceE*::Tp was adapted from that reported by Ryan and colleagues (36). Briefly, cells (300 μg) were harvested from agar plates or shaking cultures grown at 30°C in S medium for 12, 24, and 48 h. Nucleotides were extracted by resuspending the cells in water and heating at 100°C for 5 min. The extract was lyophilized, resuspended in 500 μl of water certified for high-performance liquid chromatography (HPLC) analysis, and filtered (0.2-μm pore size). Extracts equivalent to 150 μg (wt/wt) of cells were

adjusted to 500 μl in 0.1 M triethylammonium acetate (TEAA) buffer (pH 4.5) and subjected to HPLC separation. HPLC was performed on a 250- by 4.6-mm reverse-phase column (Hypersil ODS 5 μm; Hypersil-Keystone) at room temperature, with detection at 260 and 280 nm, on an ICS-U3000 IC system (Dionex, United Kingdom). Running conditions were optimized by using synthetic cyclic-di-GMP (Biolog). Runs were carried out in 0.15 M TEAA buffer (pH 4.5) at 1 ml/min, using a multistep gradient of acetonitrile. Relevant fractions of 1 ml were collected, lyophilized, and resuspended in 10 μl H_2O. For quantification, a standard curve was established whereby synthetic cyclic-di-GMP was added to relevant cell extracts. The area of the peak was used to estimate the amount of cyclic-di-GMP in a sample in reference to the wet cell weight. Quantification was further validated by mass spectrometry using matrix-assisted laser desorption ionization–time of flight analysis.

Motility tests. For the motility test, swimming plates with 0.3% (wt/vol) Bacto agar (Difco) and swarming plates with 0.5% (wt/vol) Noble agar were prepared using S medium and LB with 0.5% (wt/vol) glucose, respectively. For estimation of motility, overnight bacterial cultures (5 μl) were inoculated onto an agar surface and incubated at 30°C for 48 h, followed by colony diameter determinations.

Pellicle assay. For the pellicle assay, overnight cultures were inoculated in tubes containing 5 ml of S medium at an OD_{640} of 1.0 and kept static for 3 days at 30°C. Pellicles were assayed by visual inspection of the air-liquid interface, and the complete coverage of the surface with a cell layer was considered the extent of pellicle formation.

Cultivation of biofilms. Biofilm formation assays in microtiter plates were performed as previously described (28, 37). Biofilm formation was also studied under continuous flow conditions using the sterile Stovall 3-chamber flow cell system (Fisher Scientific). Briefly, S medium was pumped into the system for 3 h prior to inoculation of bacteria to wash and prevent system bubbles, using an Ismatec peristaltic pump. The flow chambers were inoculated by injecting in each flow channel 300-μl aliquots of the overnight cultures of *B. cepacia* IST408, *bceF*::Tp mutant, or *bceE*::Tp mutant harboring pIN25 expressing the *gfp* gene to a dilution resulting in an OD_{640} of 0.2. After inoculation, the flow channels were left without flow for 3 h, after which S medium flow was restarted at a rate of 0.4 ml/min. The flow cell system was kept at 30°C during the experiments, except during confocal microscopy analysis.

Microscopy and image analysis. Biofilm formation was examined at 48 h by scanning confocal laser microscopy on a Leica TCS SP5 inverted confocal microscope (DMI6000; Leica Microsystems CMS GmbH, Mannheim, Germany) with an argon laser for excitation. A 63× apochromatic objective with a numerical aperture of 1.2 (Zeiss, Jena, Germany) was used for all experiments. Strains under study expressed GFP, which allowed fluorescent visualization of bacterial cells. Data acquired were analyzed using the ImageJ program (http://rsbweb.nih.gov/ij/). Biomass thickness and the roughness coefficient were calculated using COMSTAT2 (http://www.comstat.dk) (38; M. Vorregaard, B. K. Ersbøll, L. Yang, J. A. J. Haagensen, S. Molin, and C. Sternberg, personal communication). The results shown were obtained using the three-dimensional (3D) viewer function and are representative of 3 independent experiments.

***Galleria mellonella* killing assays.** *B. cepacia* strains were screened for virulence in a *G. mellonella* wax moth larvae infection model as previously described (39). Larvae were injected with approximately 2×10^6 bacterial cells suspended in 10 mM $MgSO_4$ with 1.2 mg/ml ampicillin and incubated in the dark at 30°C. Control larvae were injected with 10 mM $MgSO_4$ with 1.2 mg/ml ampicillin. Larvae were scored as dead or alive for a period of 2 days. Duplicates of 10 larvae were used in each experiment, and three independent assays with different larvae generations were performed.

Microarray data accession number. Microarray data were deposited in the Gene Expression Omnibus (GEO) repository at NCBI under accession number GSE38183 (http://www.ncbi.nlm.nih.gov/geo/query/acc.cgi?acc=GSE38183).

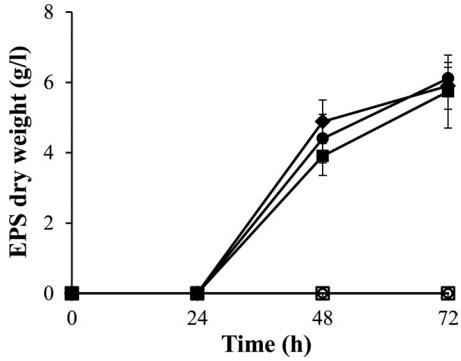

FIG 1 Exopolysaccharide production in liquid S medium at 30°C by *Burkholderia cepacia* IST408/pDA17 (◆), IST408 *bceE*::Tp/pDA17 (○), IST408 *bceE*::Tp/+p*bceE* (●), IST408 *bceF*::Tp/pDA17 (□), and IST408 *bceF*::Tp/+p*bceF* (■). The data are means ± standard deviations from the results of at least three independent experiments.

RESULTS

Gene expression profiles of mutants *bceE*::Tp and *bceF*::Tp versus wild-type *B. cepacia* IST408. Since the *bceF*::Tp mutant is unable to produce exopolysaccharide while the wild-type strain *B. cepacia* IST408 is (28), it was necessary to exclude that the possible differences for the strains were caused by the EPS directly and not by the presence/absence of the BceF kinase. Therefore, we constructed an insertion mutant for the *bceE* gene (located upstream of *bceF*) that encoded the predicted auxiliary membrane protein BceE, which is required for cepacian export. This insertion mutant, *B. cepacia* IST408 *bceE*::Tp, showed the same growth behavior as the wild-type *B. cepacia* IST408 strain and the *bceF*::Tp mutant (data not shown) and, as expected, was unable to produce cepacian (Fig. 1). In *trans* complementation of *bceE*::Tp and *bceF*::Tp mutants with the constitutive pDA17 vector harboring *bceE* (+p*bceE*) or *bceF* (+p*bceF*), respectively, restored EPS production to the wild-type level (Fig. 1).

To gain insight into the broader role of BceF tyrosine kinase, a transcriptomic approach using a custom *Burkholderia* GeneChip array was followed. Since we used *B. cepacia* IST408 as a model organism and the species represented on the array are *B. cenocepacia* J2315 and *B. multivorans* ATCC 17616 (31), there was the need to determine which individual probes representing a transcript hybridized efficiently to *B. cepacia* IST408 genomic DNA. Therefore, the genomic DNA of this bacterium was hybridized to the microarray. Setting a threshold for minimum intensity of 80 and for at least 7 probes per probe set within the software Xspecies (32), we retained 14,752 probe sets. Under these conditions, the comparison of the gene expression profile of the *bceE*::Tp mutant with that of IST408 showed 1 gene with statistically significant increased expression and 4 genes with statistically significant decreased expression (≥1.6-fold change lower confidence bound with a resulting false-discovery rate of 0%). The gene with increased expression encodes a putative metallo-beta-lactamase, and the genes with decreased expression are predicted to be involved in acetoin metabolism (see Table S2 in the supplemental material). These results confirmed that after 12 h of growth in S medium, the transcriptome of *B. cepacia* IST408 and of the *bceE*::Tp mutant derivative are very similar, and any differences between the *bceF*::Tp and IST408 transcriptomes are due to the presence/absence of the BceF kinase. The comparison of the

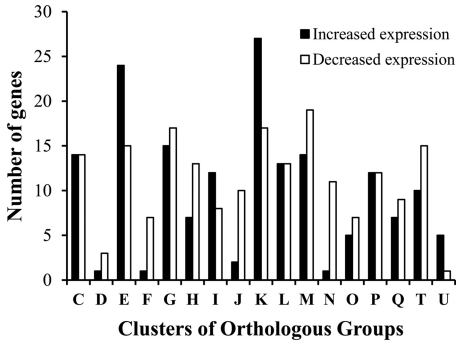

FIG 2 Number of genes with differential expression according to the major clusters of orthologous groups (COGs) categories when the *bceF*::Tp mutant was compared to wild-type *B. cepacia* IST408. A total of 630 genes with statistically significant altered expression were obtained by using a custom Affymetrix *Burkholderia* GeneChip. (C) Energy production and conversion; (D) cell division; (E) amino acid transport and metabolism; (F) nucleotide transport and metabolism; (G) carbohydrate transport and metabolism; (H) coenzyme transport and metabolism; (I) lipid transport and metabolism; (J) translation, ribosomal structure, and biogenesis; (K) transcription; (L) replication, recombination, and repair; (M) cell wall, membrane, and envelope biogenesis; (N) cell motility; (O) posttranslational modification and protein turnover; (P) inorganic ion transport and metabolism; (Q) secondary metabolite biosynthesis and transport; (T) signal transduction; (U) intracellular trafficking.

bceF::Tp mutant transcriptome with that of the wild-type *B. cepacia* IST408 strain (≥1.2-fold change lower confidence bound with a resulting false-discovery rate of ≤1.7%) showed 304 genes with statistically significant increased expression and 326 genes with statistically significant decreased expression. Almost half (43%) of the identified genes belonged to the category of poorly characterized genes or had no COG classification. Figure 2 shows the major categories of the remaining differentially expressed genes. Globally, our results indicated that in the absence of BceF tyrosine kinase, the cell's transcriptome showed a significant decrease in the expression of genes related to cell motility, stress response (universal stress proteins, heat shock proteins, proteases, etc.), and DNA replication, recombination, and repair (Table 2). In contrast the expression levels of genes encoding transcriptional regulators or lipid metabolism and genes related to cyclic-di-GMP signaling were increased in the *bceF*::Tp mutant transcriptome (Table 2). (The complete lists of differentially expressed genes are presented in Tables S3 and S4 in the supplemental material.)

To confirm the data obtained by microarray analysis, expression levels of 11 representative genes from COGs C, E, K, N, R, T, and U were analyzed by qRT-PCR. The results obtained were in good agreement with the microarray data (Table 3).

Genes involved in metabolism. Metabolic changes accounted for one-third of differentially expressed genes between the *bceF*::Tp mutant and the wild-type strain. In particular, genes involved in energy conversion, coenzyme metabolism, and amino acid metabolism had decreased expression in the *bceF*::Tp mutant, while genes related to lipid metabolism and nutrient uptake had increased expression. Among the genes with decreased expression in the *bceF*::Tp mutant, there were genes encoding glycolytic enzymes (*gapA* and BCAM0311) and the gene *pckG*, which encodes the phosphoenolpyruvate carboxykinase enzyme that removes oxaloactetate from the citrate cycle into the gluconeogenesis pathway (Table 2). The genes with decreased expression required for coenzyme metabolism are involved in the metabolism of porphyrin, thiamine, folate, ascorbate, and biotin. In the category of amino acid metabolism, we observed a 1.7- to 1.9-fold decrease in expression of the genes *gcvP* and *gcvT*, which encode two of the enzymes of the glycine cleavage system that is involved in the synthesis of one-carbon (C_1) units used in the biosynthesis of purines, methionine, and thymine and for other cellular methylation reactions.

A category of genes with increased expression in the *bceF* mutant encodes ABC transporters involved in monosaccharide, amino acid, peptide, and mineral and organic ion transport (Table 2). With regard to lipid metabolism, we observed a 1.5-fold increase in expression of the *cls* gene, which encodes cardiolipin synthetase. Cardiolipin is an anionic tetraacylphospholip found in the cytoplasmic membrane of bacteria, and it is important for optimal assembly of protein complexes, such as the electron transport complexes (40). We also observed increased expression of genes involved in fatty acid biosynthesis (BCAM2001 and BCAM2283) and decreased expression of genes for their catabolism (BCAL3191 and BCAM0142). It is thus possible that in the absence of BceF kinase, bacteria need to restructure the membrane lipid composition, perhaps to stabilize some protein complexes and/or alter permeability.

Genes involved in envelope biogenesis. Regarding cell wall biosynthesis, the gene *dadX*, which encodes a protein that catalyzes the reversible racemization of L-Ala and D-Ala, showed 2.0-fold decreased expression in the *bceF*::Tp mutant. As D-Ala is an essential component of the cell wall peptidoglycan, we cannot exclude that the *bceF*::Tp mutant may have differences in its peptidoglycan structure. Another important component of the cell wall is the lipopolysaccharide. Three genes involved in O-antigen biosynthesis and one in lipid A modification showed 1.7- to 2.4-fold increased expression in the *bceF*::Tp mutant strain. One of the genes, *wbiF*, encodes a glycosyltransferase involved in the transfer of a sugar residue to the O-antigen core oligosaccharide. The other two genes were *wzm* and *wzt*, which encode a predicted two-component ABC transporter required for O-antigen export across the plasma membrane. The last gene, with a 1.8-fold increase in expression, was BCAM1214, which encodes a protein homologue of LpxO dioxygenase enzymes from other bacteria; these enzymes are required for hydroxylation of lipid A. It is thus possible that the *bceF*::Tp mutant strain produces a different amount of and/or a modified lipopolysaccharide.

Microarray data also showed 1.6-fold decreased expression of *ompR*, which encodes the response regulator OmpR, in the *bceF*::Tp mutant. Together with the histidine kinase EnvZ, OmpR is involved in regulating outer membrane composition in several bacteria, is required for curli expression and for biofilm formation in *E. coli*, and is also involved in resistance to phagocytosis and in survival within macrophages by *Yersinia pestis* (41, 42). Although the genes regulated by EnvZ/OmpR in *Burkholderia* are unknown, we observed decreased expression of at least 9 genes encoding putative lipoproteins and outer membrane proteins in the *bceF*::Tp mutant, while only 4 showed increased expression. In addition, the *secB* gene, which encodes the preprotein translocase of the Sec pathway necessary for the export of proteins to the periplasm, outer membrane, or extracellular milieu, also showed reduced expression in the *bceF*::Tp mutant. Taken together, these observations suggest that in addition to the absence of exopolysaccharide, the *bceF*::Tp mutant must have other differences in its

TABLE 2 Differentially expressed genes for the *B. cepacia* IST408 *bceF*::Tp mutant transcriptome versus IST408, separated by functional group

Functional class	Gene identifier	LB-FC[a]	FC[b]	Gene name	Description
Cell motility	BCAL0113	−1.3	−1.5	*fliD1*	B-type flagellar hook-associated protein 2 (HAP2)
	BCAL0131	−1.2	−1.5	*tar*	Methyl-accepting chemotaxis protein
	BCAL0136	−1.2	−1.5	*cheZ*	Chemotaxis regulator CheZ
	BCAL0563	−1.3	−1.6	*flgA*	Flagellar basal body P-ring biosynthesis protein FlgA
	BCAL0564	−1.2	−1.5	*flgB*	Flagellar basal body rod protein FlgB
	BCAL0565	−1.3	−1.6	*flgC*	Flagellar basal body rod protein FlgC
	BCAL0567	−1.2	−1.7	*flgE1*	Flagellar basal body FlgE domain protein
	BCAL1531	1.3	1.6		Flp-type pilus assembly protein
	BCAL1533	1.3	1.9		Putative lipoprotein
	BCAL1677	−1.4	−1.8		Putative type 1 fimbrial protein
Envelope biogenesis	BCAL0287	−2.0	−3.1		OmpW family protein
	BCAL3122	1.3	1.7	*wbiF*	O-antigen glycosyltransferase
	BCAL3130	1.3	2.4	*wzt*	ABC transporter ATP-binding protein
	BCAL3131	1.4	1.7	*wzm*	ABC transporter, membrane permease
	BCAM1204	−1.5	−2.0	*dadX*	Alanine racemase
Replication, recombination, and repair	BCAL1204	1.5	1.9		Putative helicase
	BCAL1897	−1.4	−1.7	*recR*	Recombination protein RecR
	BCAL1963	−1.6	−2.1		DNA polymerase III, delta prime subunit
	BCAL2188	−1.3	−1.7		Putative single-stranded DNA-specific exonuclease
	BCAL3005	−1.3	−1.6		Possible DNA polymerase/helicase
	BCAL3141	−1.3	−1.6		Holliday junction resolvase-like protein
	BCAL3256	−1.2	−1.5	*mutL*	DNA mismatch repair protein MutL
	BCAM1258	−1.4	−1.6		Putative DNA-binding protein
Transcription	BCAL0562	−1.2	−1.6	*flgM*	Negative regulator of flagellin synthesis (anti-σ^{28})
	BCAL0787	−1.3	−1.8	*rpoH*	RNA polymerase factor σ^{32}
	BCAL1879	−1.3	−1.7	*hfq*	RNA-binding Hfq protein
	BCAL1538	−1.3	−1.8	*hfq2*	RNA-binding Hfq protein
	BCAL3055	−1.3	−1.6	*nusB*	Transcription antitermination protein NusB
	BCAL3151	1.5	1.7		Putative transmembrane anti-σ factor
	BCAL3178	−1.4	−1.7		LysR family regulatory protein
	BCAM0742	1.6	1.9		LysR family regulatory protein
Regulatory/signal transduction	BCAL0128	−1.2	−1.5	*cheY*	Chemotaxis two-component response regulator CheY
	BCAL0430	1.3	1.7		Putative diguanylate cyclase
	BCAL1069	−1.2	−1.5	*cdpA*	Putative cyclic-di-GMP phosphodiesterase
	BCAL2011	−1.3	−1.6	*ompR*	Osmolarity response regulator
	BCAM1162	−1.3	−1.5	*cheB3*	Chemotaxis-specific methylesterase
	BCAM1670	1.3	2.0		Putative cyclic-di-GMP signaling protein
Defense mechanisms	BCAL0389	−1.3	−1.7	*dsbC*	Thiol-disulfide interchange protein DsbC
	BCAL0807	−1.5	−2.2		ATP-dependent protease
	BCAL2119	−1.5	−2.2		Universal stress protein family protein
	BCAL2410	−1.2	−1.5		Rhodanese domain protein
	BCAL3006	−1.4	−1.8	*cspA*	Cold shock-like protein
	BCAL3147	−1.3	−1.8	*groES1*	Cochaperonin GroES
	BCAM0050	−1.3	−1.6		Universal stress protein family protein
	BCAM0278	−1.3	−1.9		Putative heat shock protein 21
	BCAM0294	−1.3	−1.8		Putative universal stress protein
	BCAM0309	1.6	1.9	*ftsH*	ATP-dependent metalloprotease FtsH
	BCAM0703	−1.3	−1.4		Putative glutathione *S*-transferase domain
	BCAM2378	−1.6	−2.0	*pepX*	X-prolyl-dipeptidyl aminotransferase
Transporters	BCAL0340	−1.2	−1.6		Putative lipoprotein (type VI)
	BCAL0341	1.2	1.6		Type VI secretion protein, VC_A0107 family
	BCAL0343	1.4	1.7	*hcp*	Type VI secretion system effector, Hcp1 family
	BCAL0348	1.3	1.5	*bcsE*	Type VI secretion-associated protein, ImpA family
	BCAL0350	−1.3	−1.9		Hypothetical protein BCAL0350 (type VI secretion)
	BCAL0742	−1.2	−1.5	*secB*	Preprotein translocase subunit SecB
	BCAL1646	1.4	2.0		Putative oligosaccharide ABC transporter protein
	BCAL3099	1.3	1.6		Putative branched-chain amino acid transport, permease
	BCAM0760	1.5	1.7	*hisQ*	Histidine transport system permease
	BCAM0769	1.3	1.5		Ribose transport system permease protein
Energy conversion	BCAL3342	1.3	1.6		Phosphoglycerate mutase
	BCAL3388	−1.3	−1.6	*gapA*	Glyceraldehyde 3-phosphate dehydrogenase 1
	BCAM0311	−1.2	−1.6		Putative 6-phosphofructokinase
	BCAM1581	−1.4	−1.9	*pckG*	Phosphoenolpyruvate carboxykinase (GTP)
Amino acid metabolism	BCAL0073	−1.4	−1.7	*gcvP*	Glycine dehydrogenase
	BCAL0075	−1.5	−1.9	*gcvT*	Glycine cleavage system aminomethyltransferase T
	BCAL0632	−1.5	−2.0		Putative dehydrogenase
	BCAM0011	−1.5	−1.7	*tdh*	L-Threonine 3-dehydrogenase

(Continued on following page)

TABLE 2 (Continued)

Functional class	Gene identifier	LB-FC[a]	FC[b]	Gene name	Description
Lipid metabolism	BCAL0845	1.2	1.7	*acpP*	Acyl carrier protein
	BCAL0992	−1.2	−1.6	*fabH2*	3-Oxoacyl-(acyl carrier protein) synthase III
	BCAL2105	1.2	1.5	*cls*	Cardiolipin synthetase
	BCAL2322	1.3	1.5		Enoyl coenzyme A hydratase
	BCAL3191	−1.2	−1.7		Putative glutaryl coenzyme A dehydrogenase
	BCAM0142	−1.2	−1.4		Putative acyl coenzyme A dehydrogenase family protein
	BCAM1214	1.4	1.8		Putative dioxygenase
	BCAM2001	1.3	1.4		Short-chain dehydrogenase reductase
	BCAM2283	1.2	1.6		Short-chain dehydrogenase
	BCAM2568	−1.4	−1.7		Beta-ketoadipyl–coenzyme A thiolase
Coenzyme and inorganic ion transport and metabolism	BCAL0040	−1.4	−1.7	*hemE*	Uroporphyrinogen decarboxylase
	BCAL0475	−1.2	−1.6		Putative 6-pyruvoyl tetrahydropterin synthase
	BCAL0665	−1.5	−1.7	*bioD*	Dithiobiotin synthetase
	BCAL1043	−1.3	−1.6	*gudD*	Glucarate dehydratase
	BCAL1047	−1.2	−1.5	*pdxY*	Pyridoxamine kinase
	BCAL1728	−1.3	−1.6	*cbiD*	Cobalt precorrin 6A synthase
	BCAL2112	−1.2	−1.5	*thiD*	Phosphomethylpyrimidine kinase
	BCAL2458	1.6	2.0	*rubA*	Rubredoxin-type $Fe(Cys)_4$ protein
	BCAL2782	−1. 3	−1.7	*pdxH*	Pyridoxamine 5′-phosphate oxidase
	BCAL3049	−1.2	−1.6	*hemL*	Glutamate-1-semialdehyde 2,1-aminomutase
	BCAL3094	−1.5	−2.2	*hemN*	Coproporphyrinogen III oxidase
	BCAM2626	1.3	1.6	*huvA*	Putative heme receptor protein
Nucleotide metabolism	BCAL0012	−1.5	−1.9		Adenylate cyclase
	BCAL0635	−1.3	−1.5	*yagT*	Putative xanthine dehydrogenase iron-sulfur binding subunit
	BCAL3140	−1.2	−1.5	*pyrR*	Bifunctional pyrimidine regulatory protein PyrR uracil phosphoribosyltransferase
	BCAL3172	−1.4	−1.8	*xdhB*	Xanthine dehydrogenase, molybdopterin-binding subunit
	BCAL3400	−1.2	−1.6	*pyrF*	Orotidine 5′-phosphate decarboxylase

[a] LB-FC, lower bound of fold change.
[b] FC, fold change.

cell wall that affect permeability or interactions with the surrounding environment.

Mutation of the *bceF* gene suggests a role for it in the response to stress. In our data set, the gene *rpoH* encoding the sigma 32 alternative sigma factor showed 1.8-fold decreased expression in the *bceF*::Tp mutant compared with the IST408 wild-type strain. RpoH mediates the heat shock response, but it is also activated under conditions that destabilize folded proteins or make correct nascent protein folding more difficult (43). The comparison of our data with genes that are known to be regulated by RpoH in *E. coli* (43) revealed many with decreased expression in the *bceF*::Tp mutant (Table 2). These genes encode chaperones GroES1 and HSP21, the *dsbC* genem which encodes a protein involved in disulfide bond formation, several genes that encode universal stress-related proteins, and genes encoding putative proteases. The RpoH regulon also encodes proteins involved in cofactor biosynthesis and iron-sulfur assembly (43) and, as we described above, several genes involved in cofactor biosynthesis showed decreased expression. Another function of the RpoH regulon is the protection of DNA and RNA. Hence, we observed a decreased expression of genes involved in the repair of DNA lesions (*recR* and *mutL*) in the *bceF*::Tp mutant, as well as a predicted Holliday junction resolvase-like protein (BCAL3141), a specific single-stranded DNA-specific exonuclease (BCAL2188), and the cold shock protein gene *cspA*. Also, gene *nusB*, whose product binds to RNA polymerase to alleviate the effects of supercoiling on transcription, and the RNA chaperone-encoding genes *hfq* and *hfq2* showed decreased expression in the *bceF*::Tp mutant. To determine whether the decreased expression of the putative RpoH and its regulon members is relevant under heat shock conditions, wild-type IST408 and the *bceE*::Tp and *bceF*::Tp mutants and the complemented mutants were incubated at 50°C for 20 min, and CFU were counted at several time points (Fig. 3A). The results obtained showed a more sensitive phenotype for the *bceF*::Tp mutant, with the cells having a lower survival rate under heat stress. In *trans* complementation of the *bceF*::Tp mutant with the pDA17 vector containing the *bceF* or *rpoH* genes rescued its heat-sensitive phenotype (Fig. 3A). When cells were exposed to UV light for a period of time, we also observed a decrease in the survival rate of the *bceF*::Tp mutant compared to the *bceE*::Tp and wild-type *B. cepacia*, which was rescued by the introduction of *bceF* or *rpoH* genes carried by pDA17 (Fig. 3B).

TABLE 3 Quantitative real-time RT-PCR analysis results for the *B. cepacia* IST408 wild-type strain and *bceE*::Tp and *bceF*::Tp isogenic mutant derivatives

Comparison and gene identifier (gene name)	Microarray LB-FC (FC)[a]	Real-time fold change ± SD
bceF::Tp vs IST408		
BCAL0073 (*gcvP*)	−1.4 (−1.7)	−1.5 ± 0.4
BCAL0564 (*flgB*)	−1.2 (−1.5)	−1.7 ± 1.2
BCAL0787 (*rpoH*)	−1.3 (−1.8)	−1.9 ± 0.1
BCAL1677	−1.4 (−1.8)	−4.0 ± 0.2
BCAL2011 (*ompR*)	−1.3 (−1.6)	−1.9 ± 0.2
BCAL1531	1.3 (1.6)	1.2 ± 0.3
BCAL3486	1.2 (1.4)	3.1 ± 0.1
BCAM2054 (*bcscD*)	1.4 (1.8)	2.3 ± 0.1
BCAM2348	1.5 (1.6)	2.1 ± 0.1
bceE::Tp vs IST408		
BCAL1910 (*acoB*)	−1.8 (−2.6)	−1.9 ± 0.4
BCAM2378 (*pepX*)	−1.7 (−2.3)	−1.8 ± 0.1

[a] LB-FC, lower bound of fold change; FC, fold change.

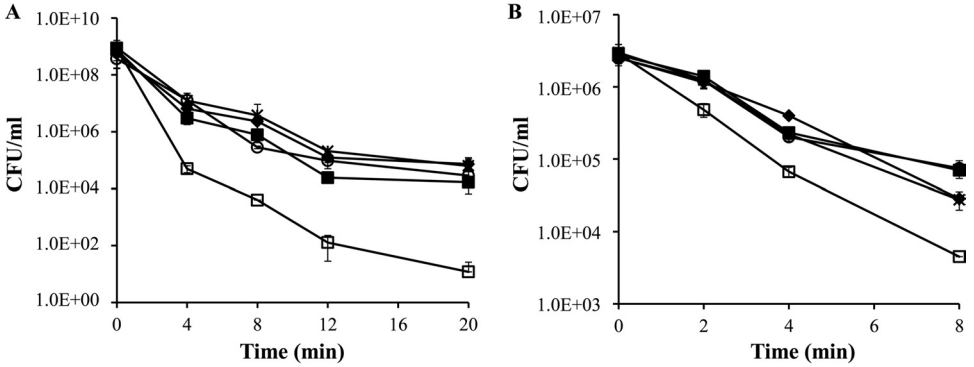

FIG 3 Bacterial survival under heat and UV light stresses. Cells of *B. cepacia* IST408/pDA17 (◆), IST408 *bceE*::Tp/pDA17 (○), IST408 *bceF*::Tp/pDA17 (□), IST408 *bceF*::Tp/+p*bceF* (■), and IST408 *bceF*::Tp/+p*rpoH* (✳) were incubated at 50°C (A) or under UV light exposure (B), and CFU determinations were made by plating the cells in LB medium at 30°C. The data are means ± standard deviations from the results of at least three independent experiments.

Although the RpoH regulon is also induced by oxidative stress, the only two genes with a putative role in antagonizing this type of stress and that showed decreased expression in the *bceF*::Tp mutant were BCAM0703, which encodes a putative glutathione *S*-transferase, and BCAL2410, which encodes a protein with a rhodanese domain (Table 2). Despite that, no differences were found between the wild-type strain and the mutants with respect to growth inhibition in the presence of oxidative stress agents, such as H_2O_2 or cumene hydroperoxide (data not shown).

Mutation of *bceF* affects motility and biofilm formation. Analysis of gene expression levels in the flagellar regulon indicated 1.5-fold decreased expression in the *bceF*::Tp mutant of the *cheY*, *cheB3*, *cheZ*, and *tar* genes, whose products are involved in chemotaxis. In addition, the filament cap-encoding gene *fliD1*, the flagellar basal body-encoding genes *flgABCE1*, and *flgM*, which encodes the negative regulator of flagellin synthesis also displayed decreased expression in the *bceF*::Tp mutant (Table 2). To test whether differences in the expression of these genes led to a phenotype in semisolid medium, the swimming and swarming abilities of the strains were performed. Consistent with the gene expression data, we observed that after 24 h of incubation the *bceF*::Tp mutant displayed lower swimming and swarming motilities than the wild-type strain and the *bceE*::Tp mutant, but these phenotypes were complemented by the expression of the *bceF* gene from pDA17 (Fig. 4).

We also compared cell-to-cell adhesion in wild-type bacteria and in the *bceE*::Tp and *bceF*::Tp mutants by using static broth cultures. The results showed that broth cultures of the wild-type strain remained visibly clear after 3 days of incubation, with clumping of the bacterial cells at the bottom of the culture tube (Fig. 5A). For this property, the *bceE*::Tp mutant showed an intermediate phenotype, and the broth culture of the *bceF*::Tp mutant showed mainly bacterial cells in suspension (Fig. 5A). Pellicle formation at the air-liquid interface was mainly observed in the wild-type IST408 and, to a lesser extent, in both mutants (Fig. 5A). Since pellicle formation is indicative of the production of an adhesive matrix, we first investigated biofilm formation under static conditions by measuring cell adhesion to an abiotic surface based on crystal violet staining. The *bceF*::Tp mutant biofilm at 48 h retained 2.0- and 1.3-fold less crystal violet than the biofilm of wild-type *B. cepacia* IST408 and the *bceE*::Tp mutant, respectively (Fig. 5B). Both mutant phenotypes were restored by expressing in *trans* from pDA17 the mutant strain defective gene. We also tested biofilm formation in continuous flow cells by constitutively expressing GFP from a plasmid in the three strains. After a 48-hour period, *B. cepacia* IST408 biofilms showed well-differentiated microcolonies with shapes resembling early cauliflower-like structures (Fig. 5C). The *bceE*::Tp mutant formed cell aggregates that covered more than 50% of the optical field, but without forming 3D macrocolonies as thick as the ones observed for the wild-type strain, with maximum thicknesses of 7.76 and 4.12 μm for the wild-type and *bceE*::Tp mutant, respectively. In contrast, the *bceF*::Tp mutant seemed to be unable to form mature biofilm forms, presenting small and scarce colonies throughout the chamber surface with a maximum thickness for this biofilm of 2.74 μm (Fig. 5C). The biomass contained in each strain's biofilm was also evaluated using COMSTAT2, with the parental IST408 biofilms having a biomass volume-to-surface ratio of 6.61 $\mu m^3/\mu m^2$, the *bceE*::Tp mutant with 3.45 $\mu m^3/\mu m^2$, and the *bceF*::Tp mutant with 2.53 $\mu m^3/\mu m^2$, which is consistent with the biofilm formation data obtained using crystal violet staining.

Inactivation of the *bceF* gene increases the production of cyclic-di-GMP. Microarray data showed the altered expression of

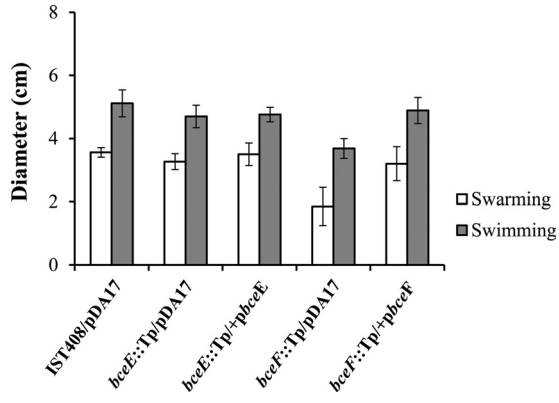

FIG 4 Swimming and swarming motilities of wild-type *B. cepacia* IST408, *bceE* and *bceF* mutants, and complemented mutants. Plates containing 0.3% and 0.6% purified agar were used to test swimming and swarming motilities, respectively. Plates were spotted with 5-μl of mid-exponential-phase *B. cepacia* cultures previously grown in S medium for 12 h at 30°C, and the size of each halo was measured. The data are means ± standard deviations from the results of at least three independent experiments.

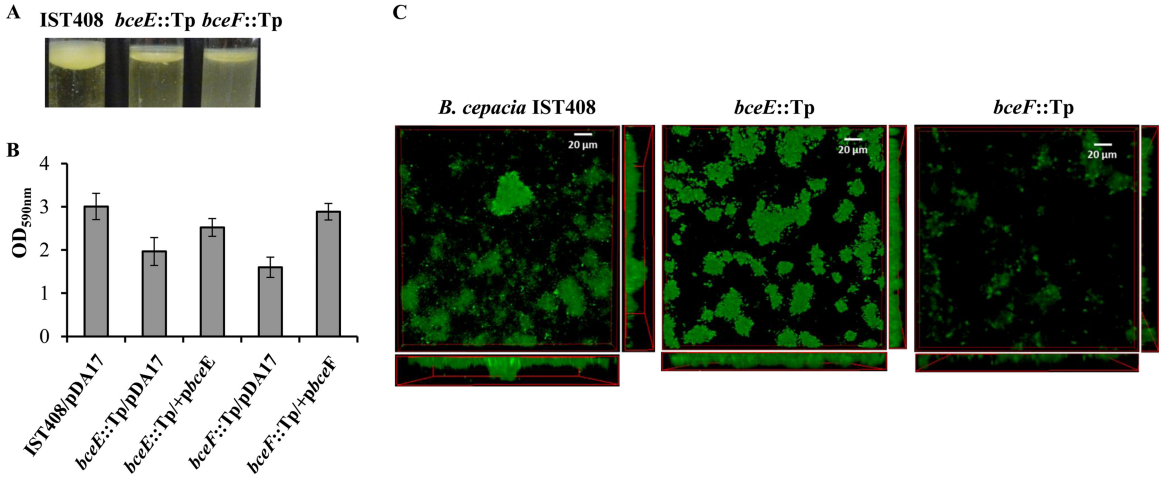

FIG 5 Effects of *bceE* and *bceF* mutations on biofilm formation. (A) Pellicle formation in a static S medium liquid culture of *B. cepacia* IST408 and isogenic mutants *bceE*::Tp and *bceF*::Tp. (B) Biofilm formation measured by crystal violet staining in an assay using static broth cultures of *B. cepacia* IST408, the *bceE*::Tp/pDA17 and *bceF*::Tp/pDA17 mutants, and both complemented mutants. Bacteria were cultured in S medium in a 96-well microplate for 48 h and measured spectroscopically at a 590-nm wavelength. The data are means ± standard deviations from the results of at least three independent experiments. (C) Scanning confocal photomicrographs of surface-attached communities formed by *B. cepacia* IST408 wild type and the isogenic mutants *bceE*::Tp and *bceF*::Tp labeled with GFP. The biofilms were grown in flowthrough continuous culture reaction vessels for 48 h at 30°C in S medium. Shown in the right and lower frames are vertical sections through the biofilms. Bar, 20 μm.

genes BCAL1069, BCAL0430, and BCAM1670, which are putatively involved in cyclic-di-GMP signaling (Table 2). Genes BCAL0430 and BCAM1670, encoding putative cyclic-di-GMP diguanylate cyclases with a GGDEF domain, showed 1.7- to 2.0-fold increased expression in the *bceF*::Tp mutant. In contrast, gene BCAL1069, which encodes a putative cyclic-di-GMP phosphodiesterase, showed 1.5-fold decreased expression. As an overview, the genome of *B. cenocepacia* J2315 has at least 25 genes involved in cyclic-di-GMP production and turnover. Therefore, it is difficult to predict whether changes in the expression of genes encoding digualylate cyclases and phosphodiesterases will have an effect on the cyclic-di-GMP concentration. To assess whether BCAL1069, BCAL0430, and BCAM1670 gene products are relevant in the regulation of intracellular cyclic-di-GMP levels in *B. cepacia*, this secondary messenger was extracted from cells of the wild-type IST408 and *bceE*::Tp and *bceF*::Tp mutants at 12, 24, and 48 h of growth in S medium (Fig. 6). The intracellular level of cyclic-di-GMP in the wild-type IST408 and *bceE*::Tp mutant did not change over the 48-h test period, with the mutant showing a slightly higher concentration. In contrast, the *bceF*::Tp mutant showed at least a 4-fold increase of cyclic-di-GMP levels above the wild-type *B. cepacia* IST408 in the first 24 h, with the concentration dropping to levels similar to the *bceE*::Tp mutant but still 2-fold higher than in the IST408 strain (Fig. 6).

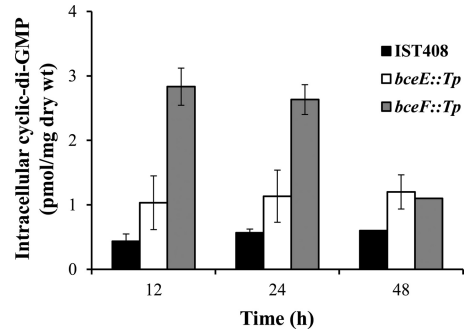

FIG 6 Intracellular cyclic-di-GMP contents in wild-type *B. cepacia* IST408 and the *bceE*::Tp and *bceF*::Tp mutants. Intracellular nucleotides were extracted at 12, 24, and 48 h of growth, and the cyclic-di-GMP content was measured by reverse-phase HPLC. The amount of cyclic-di-GMP is shown per milligram (dry weight) of cells. The data are means ± standard deviations from the results of at least three independent experiments.

The *bceF* gene plays a role in virulence. Mutation in the *bceF* gene affected diverse phenotypes, such as motility, resistance to stress, and biofilm formation, among others. Due to the importance of these phenotypes in *B. cepacia* virulence, we determined whether the *bceF*::Tp mutant could also be attenuated in virulence by using *Galleria mellonella* as an acute infection model. This was accomplished by injecting approximately 2×10^6 CFU of each bacterial strain into larvae. The results indicated virulence attenuation by the *bceF*::Tp mutant, with 35% of the larvae being alive at 48 h postinfection, while in the presence of the *bceE*::Tp mutant and the wild-type IST408 almost all larvae were dead (Fig. 7). Complementation of the *bceF*::Tp mutant with pDA17 expressing the *bceF* gene restored virulence to the wild-type level. These data regarding virulence attenuation of the *bceF*::Tp mutant are consistent with the decreased expression of genes putatively involved in virulence as well as the observed phenotypic properties.

DISCUSSION

In this work we performed global gene expression analysis and a series of *in vivo* experiments looking for phenotypes of a *B. cepacia* strain with an inactivated *bceF* gene encoding a BY-kinase primarily involved in cepacian exopolysaccharide biosynthesis. The results showed a remarkable effect on the number of genes differentially expressed between the wild-type and mutant strains. Considering that BceF activity is expected to be mainly at the protein level, its effect on gene expression regulation might be an indirect one. Nevertheless, these changes in gene expression have many consequences at the phenotype level, as observed for exopo-

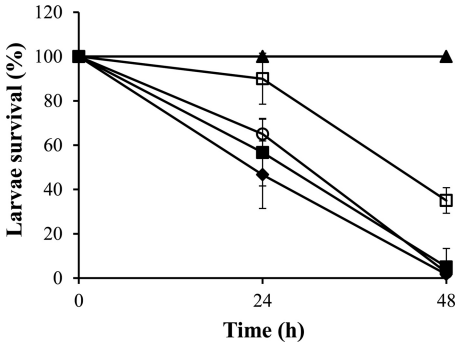

FIG 7 BceF influences the ability of *B. cepacia* IST408 to kill *G. mellonella*. Larvae were infected with approximately 2×10^6 cells of IST408/pDA17 (◆), *bceE*::Tp/pDA17 (○), *bceF*::Tp/pDA17 (□), and *bceF*::Tp/+p*bceF* (■). The control experiment without bacteria is also shown (▲). The data are means ± standard deviations from the results of at least three independent experiments.

lysaccharide production, resistance to stress, motility, biofilm formation, and virulence. Another finding from this work is that the lack of BceF activity is not compensated by other BY-kinases predicted to be present in *Burkholderia*. Effectively, our search of several Bcc sequenced genomes for BceF homologues indicated that, in addition to BceF homologues, most of them encode another putative BY-kinase, described by Fazli and collaborators to be involved in the biosynthesis of a new polysaccharide (26). *B. cenocepacia* J2315 is an exception, having two extra BY-kinases besides BceF, namely, BCAM0207 and BCAM1331.

Consistent with the decreased expression of genes involved in DNA repair and response to stress, *B. cepacia* cells lacking the BceF protein were more susceptible to stress imposed by exposure to UV irradiation or heat shock. The role of tyrosine phosphorylation in the regulation of responses to stress in *E. coli* and *B. subtilis* has been reported. The *B. subtilis* mutant in the PtkA BY-kinase was slightly less resistant than the wild-type strain when exposed to gamma irradiation-induced DNA lesions (44). As the single-strand-binding protein SsbA from *B. subtilis* is a tyrosine phosphorylation target, those authors suggested the need for PtkA (and the phosphatase PtpZ) to coordinate a cycle of SsbA coming on and off the single-stranded DNA template during repair (44), which would explain the more sensitive phenotype to radiation stress. With regard to heat shock stress, the role of tyrosine phosphorylation/dephosphorylation in the control of RpoH and RseA activities has also been previously described (9). In that work, the authors demonstrated that RpoH was phosphorylated at amino acid position 260 and that this phosphorylation event attenuated RpoH activity by inhibiting its ability to initiate transcription as a sigma factor. Our expression data indicate that in the absence of BceF tyrosine kinase, expression of both the *rpoH* gene and some of its putative regulon members decreased. Although it cannot be excluded that there is a possible effect of tyrosine phosphorylation on RpoH activity, our data point toward a reduction in the expression of the *rpoH* gene as the main cause for the lower fitness of the mutant under stress conditions. Effectively, when extra copies of the *rpoH* gene were introduced into the *bceF* mutant, both UV and heat shock resistance increased to wild-type levels.

Another line of investigation was focused on the effect of the absence of BceF on motility, biofilm formation, cyclic-di-GMP synthesis, and virulence. These are complex phenotypes with different levels of regulation and are difficult to attribute to a single factor. In a recent work, Fazli and colleagues characterized a transcriptional regulator of the CRP/FNR superfamily (BCAM1349) from *B. cenocepacia* J2315 that is able to bind cyclic-di-GMP (45). This transcriptional regulator was shown to regulate the expression of genes required for the synthesis of cellulose and fimbriae, as it was involved in biofilm formation and virulence of *B. cenocepacia* in response to the level of cyclic-di-GMP. Also in *Burkholderia pseudomallei*, the presence of higher intracellular cyclic-di-GMP levels in a phosphodiesterase *cdpA*-null mutant was associated with an absence of flagella and swimming motility and increased biofilm formation (46). According to these previous observations, the lower motility displayed by the *bceF*::Tp mutant could be a consequence of the higher levels of cyclic-di-GMP in this mutant. With regard to biofilm formation, our results showed an opposite effect, since the *bceF*::Tp mutant strain had higher levels of cyclic-di-GMP but nevertheless showed less biofilm formation. Certainly the level of cyclic-di-GMP and the transcriptional control dependent on this secondary messenger are not the only factors for biofilm formation. It has been shown with *E. coli* K-12 that the EnvZ-OmpR two-component regulatory system also controls both fimbriae and biofilm formation (42). Both OmpR and fimbria-encoding genes showed decreased expression in the *bceF* mutant, and this could perhaps explain the inability of the mutant to form biofilms with a size comparable to the wild-type *B. cepacia*. In addition, posttranslational modifications are also involved in the control of biofilm formation, namely, phosphorylation of protein tyrosine residues. A *B. subtilis* strain harboring the PtkA tyrosine kinase with mutations affecting kinase activity was unable to develop the complex radial structures typical of a maturing wild-type biofilm (47). Nevertheless, the targets controlled by these BY-kinases with direct involvement in biofilm formation are unknown.

With regard to virulence, protein phosphorylation is often directly involved in this process, as it controls the expression of virulence genes and the synthesis of macromolecules from the bacterial cell wall and also interferes directly with host signaling (48). The *B. cepacia bceF*::Tp mutant was clearly less virulent than the wild-type strain in the acute infection model with *G. mellonella* used in this work and also in a mouse infection model (29). Several factors can contribute to this virulence attenuation in the absence of the BceF protein. One of them could be related to altered membrane permeability and cell envelope composition, as suggested by experiments involving differential expression of genes related to lipid metabolism and cell wall polymer biosynthesis. These changes may have a strong impact on the modulation of the host immune response. Another reason could be the different abilities to attach to host tissues due to differential expression of pili, fimbriae, flagella, or other proteins important in this process. For example, the chaperone GroEL from *Salmonella enterica* serovar Typhimurium and *Clostridium difficile* has been experimentally demonstrated to participate in adhesion to eukaryotic cells (49, 50). Therefore, the decreased expression of genes encoding heat shock proteins and other RpoH regulon members, together with the reduced ability of *Burkholderia* to withstand stress conditions, suggests that upon encountering a stressful environment during host infection, the cells may become less proficient for survival within the host. In addition, the BceF protein may indirectly interfere with host signaling by being involved in the activation and

secretion of some effector protein for which, in its absence, cells would be less virulent.

Taken together, the *bceF* mutant seems to have complex pleiotropic phenotypes related to polysaccharide synthesis, metabolism, stress response, signaling, and biofilm formation, among others. This reflects the importance of protein phosphorylation, in particular the tyrosine kinase BceF from *Burkholderia*, in the regulation of key metabolic processes and virulence. The next aim is to identify cellular targets of this BY-kinase that could explain the observed differences at the gene expression and phenotypic levels.

ACKNOWLEDGMENTS

We acknowledge Sean May from University of Nottingham, United Kingdom, for his help with the Xspecies software.

This work was supported by FEDER and Fundação para a Ciência e a Tecnologia, Portugal (contracts PTDC/BIA-MIC/66977/2006 and PTDC/QUI-BIQ/118260/2010 to L.M.M.), a postdoctoral grant to A.S.F., and a doctoral grant to I.N.S. A.S.F. acknowledges a scholarship from Fundação Calouste Gulbenkian.

REFERENCES

1. **Grangeasse C, Terreux R, Nessler S.** 2010. Bacterial tyrosine-kinases: structure-function analysis and therapeutic potential. Biochim. Biophys. Acta **1804**:628–634.
2. **Lee DC, Jia Z.** 2009. Emerging structural insights into bacterial tyrosine kinases. Trends Biochem. Sci. **34**:351–357.
3. **Bechet E, Guiral S, Torres S, Mijakovic I, Cozzone AJ, Grangeasse C.** 2009. Tyrosine-kinases in bacteria: from a matter of controversy to the status of key regulatory enzymes. Amino Acids **37**:499–507.
4. **Lacour S, Bechet E, Cozzone AJ, Mijakovic I, Grangeasse C.** 2008. Tyrosine phosphorylation of the UDP-glucose dehydrogenase of Escherichia coli is at the crossroads of colanic acid synthesis and polymyxin resistance. PLoS One **3**:e3053. doi:10.1371/journal.pone.0003053.
5. **Mijakovic I, Poncet S, Boel G, Maze A, Gillet S, Jamet E, Decottignies P, Grangeasse C, Doublet P, Le Marechal P, Deutscher J.** 2003. Transmembrane modulator-dependent bacterial tyrosine kinase activates UDP-glucose dehydrogenases. EMBO J. **22**:4709–4718.
6. **Minic Z, Marie C, Delorme C, Faurie JM, Mercier G, Ehrlich D, Renault P.** 2007. Control of EpsE, the phosphoglycosyltransferase initiating exopolysaccharide synthesis in Streptococcus thermophilus, by EpsD tyrosine kinase. J. Bacteriol. **189**:1351–1357.
7. **Lin MH, Hsu TL, Lin SY, Pan YJ, Jan JT, Wang JT, Khoo KH, Wu SH.** 2009. Phosphoproteomics of Klebsiella pneumoniae NTUH-K2044 reveals a tight link between tyrosine phosphorylation and virulence. Mol. Cell. Proteomics **8**:2613–2623.
8. **Soulat D, Grangeasse C, Vaganay E, Cozzone AJ, Duclos B.** 2007. UDP-acetyl-mannosamine dehydrogenase is an endogenous protein substrate of Staphylococcus aureus protein-tyrosine kinase activity. J. Mol. Microbiol. Biotechnol. **13**:45–54.
9. **Klein G, Dartigalongue C, Raina S.** 2003. Phosphorylation-mediated regulation of heat shock response in Escherichia coli. Mol. Microbiol. **48**:269–285.
10. **Kolot M, Gorovits R, Silberstein N, Fichtman B, Yagil E.** 2008. Phosphorylation of the integrase protein of coliphage HK022. Virology **375**:383–390.
11. **Mijakovic I, Petranovic D, Macek B, Cepo T, Mann M, Davies J, Jensen PR, Vujaklija D.** 2006. Bacterial single-stranded DNA-binding proteins are phosphorylated on tyrosine. Nucleic Acids Res. **34**:1588–1596.
12. **Macek B, Gnad F, Soufi B, Kumar C, Olsen JV, Mijakovic I, Mann M.** 2008. Phosphoproteome analysis of E. coli reveals evolutionary conservation of bacterial Ser/Thr/Tyr phosphorylation. Mol. Cell. Proteomics **7**:299–307.
13. **Macek B, Mijakovic I, Olsen JV, Gnad F, Kumar C, Jensen PR, Mann M.** 2007. The serine/threonine/tyrosine phosphoproteome of the model bacterium Bacillus subtilis. Mol. Cell. Proteomics **6**:697–707.
14. **Eymann C, Becher D, Bernhardt J, Gronau K, Klutzny A, Hecker M.** 2007. Dynamics of protein phosphorylation on Ser/Thr/Tyr in Bacillus subtilis. Proteomics **7**:3509–3526.
15. **Misra SK, Milohanic E, Aké F, Mijakovic I, Deutscher J, Monnet V, Henry C.** 2011. Analysis of the serine/threonine/tyrosine phosphoproteome of the pathogenic bacterium Listeria monocytogenes reveals phosphorylated proteins related to virulence. Proteomics **11**:4155–4165.
16. **Sun X, Ge F, Xiao CL, Yin XF, Ge R, Zhang LH, He QY.** 2010. Phosphoproteomic analysis reveals the multiple roles of phosphorylation in pathogenic bacterium Streptococcus pneumoniae. J. Proteome Res. **9**:275–282.
17. **Ravichandran A, Sugiyama N, Tomita M, Swarup S, Ishihama Y.** 2009. Ser/Thr/Tyr phosphoproteome analysis of pathogenic and non-pathogenic Pseudomonas species. Proteomics **9**:2764–2775.
18. **Mijakovic I, Macek B.** 2012. Impact of phosphoproteomics on studies of bacterial physiology. FEMS Microbiol. Rev. **36**:877–892.
19. **Ge R, Shan W.** 2011. Bacterial phosphoproteomic analysis reveals the correlation between protein phosphorylation and bacterial pathogenicity. Genomics Proteomics Bioinformatics **9**:119–127.
20. **Jers C, Pedersen MM, Paspaliari DK, Schütz W, Johnsson C, Soufi B, Macek B, Jensen PR, Mijakovic I.** 2010. Bacillus subtilis BY-kinase PtkA controls enzyme activity and localization of its protein substrates. Mol. Microbiol. **77**:287–299.
21. **Isles A, Maclusky I, Corey M, Gold R, Prober C, Fleming P, Levison H.** 1984. Pseudomonas cepacia infection in cystic fibrosis: an emerging problem. J. Pediatr. **104**:206–210.
22. **Richau JA, Leitão JH, Correia M, Lito L, Salgado MJ, Barreto C, Cescutti P, Sá-Correia I.** 2000. Molecular typing and exopolysaccharide biosynthesis of Burkholderia cepacia isolates from a Portuguese cystic fibrosis center. J. Clin. Microbiol. **38**:1651–1655.
23. **Zlosnik JE, Hird TJ, Fraenkel MC, Moreira LM, Henry DA, Speert DP.** 2008. Differential mucoid exopolysaccharide production by members of the Burkholderia cepacia complex. J. Clin. Microbiol. **46**:1470–1473.
24. **Ferreira AS, Leitão JH, Silva IN, Pinheiro PF, Sousa SA, Ramos CG, Moreira LM.** 2010. Distribution of cepacian biosynthesis genes among environmental and clinical Burkholderia strains and role of cepacian exopolysaccharide in resistance to stress conditions. Appl. Environ. Microbiol. **76**:441–450.
25. **Ferreira A, Silva I, Oliveira V, Cunha R, Moreira L.** 2011. Insights into the role of extracellular polysaccharides in Burkholderia adaptation to different environments. Front. Cell. Infect. Microbiol. **1**:00016. doi:10.3389/fcimb.2011.00016.
26. **Fazli M, McCarthy Y, Givskov M, Ryan RP, Tolker-Nielsen T.** 2012. The exopolysaccharide gene cluster Bcam1330-Bcam1341 is involved in Burkholderia cenocepacia biofilm formation, and its expression is regulated by c-di-GMP and Bcam1349. MicrobiologyOpen doi:10.1002/mbo3.61.
27. **Moreira LM, Videira PA, Sousa SA, Leitão JH, Cunha MV, Sá-Correia I.** 2003. Identification and physical organization of the gene cluster involved in the biosynthesis of Burkholderia cepacia complex exopolysaccharide. Biochem. Biophys. Res. Commun. **312**:323–333.
28. **Ferreira AS, Leitão JH, Sousa SA, Cosme AM, Sá-Correia I, Moreira LM.** 2007. Functional analysis of Burkholderia cepacia genes bceD and bceF, encoding a phosphotyrosine phosphatase and a tyrosine autokinase, respectively: role in exopolysaccharide biosynthesis and biofilm formation. Appl. Environ. Microbiol. **73**:524–534.
29. **Sousa SA, Ulrich M, Bragonzi A, Burke M, Worlitzsch D, Leitão JH, Meisner C, Eberl L, Sá-Correia I, Döring G.** 2007. Virulence of Burkholderia cepacia complex strains in gp91$^{phox-/-}$ mice. Cell. Microbiol. **9**:2817–2825.
30. **Sambrook J, Russell DW.** 2001. Molecular cloning: a laboratory manual, 3rd ed. Cold Spring Harbor Laboratory Press, Cold Spring Harbor, NY.
31. **Silva IN, Ferreira AS, Becker JD, Zlosnik JEA, Speert DP, He J, Mil-Homens D, Moreira LM.** 2011. Mucoid morphotype variation of Burkholderia multivorans during chronic cystic fibrosis lung infection is correlated with changes in metabolism, motility, biofilm formation and virulence. Microbiology **157**:3124–3137.
32. **Hammond JP, Broadley MR, Craigon DJ, Higgins J, Emmerson ZF, Townsend HJ, White PJ, May ST.** 2005. Using genomic DNA-based probe-selection to improve the sensitivity of high-density oligonucleotide arrays when applied to heterologous species. Plant Methods **1**:10. doi:10.1186/1746-4811-1-10.
33. **Li C, Wong WH.** 2001. Model-based analysis of oligonucleotide arrays: model validation, design issues and standard error application. Genome Biol. **2**:RESEARCH0032. doi:10.1186/gb-2001-2-8-research0032.
34. **Li C, Wong WH.** 2001. Model-based analysis of oligonucleotide arrays:

expression index computation and outlier detection. Proc. Natl. Acad. Sci. U. S. A. **98**:31–36.
35. **Pfaffl MW.** 2001. A new mathematical model for relative quantification in real-time RT-PCR. Nucleic Acids Res. **29**:e45. doi:10.1093/nar/29.9.e45.
36. **Ryan RP, Lucey J, O'Donovan K, McCarthy Y, Yang L, Tolker-Nielsen T, Dow JM.** 2009. HD-GYP domain proteins regulate biofilm formation and virulence in Pseudomonas aeruginosa. Environ. Microbiol. **11**:1126–1136.
37. **Cunha MV, Sousa SA, Leitão JH, Moreira LM, Videira PA, Sá-Correia I.** 2004. Studies on the involvement of the exopolysaccharide produced by cystic fibrosis-associated isolates of the Burkholderia cepacia complex in biofilm formation and in persistence of respiratory infections. J. Clin. Microbiol. **42**:3052–3058.
38. **Heydorn A, Nielsen AT, Hentzer M, Sternberg C, Givskov M, Ersbøll BK, Molin S.** 2000. Quantification of biofilm structures by the novel computer program COMSTAT. Microbiology **146**:2395–2407.
39. **Seed KD, Dennis JJ.** 2008. Development of Galleria mellonella as an alternative infection model for the Burkholderia cepacia complex. Infect. Immun. **76**:1267–1275.
40. **Zhou P, Hu R, Chandan V, Kuolee R, Liu X, Chen W, Liu B, Altman E, Li J.** 2012. Simultaneous analysis of cardiolipin and lipid A from Helicobacter pylori by matrix-assisted laser desorption/ionization time-of-flight mass spectrometry. Mol. Biosyst. **8**:720–725.
41. **Gao H, Zhang Y, Han Y, Yang L, Liu X, Guo Z, Tan Y, Huang X, Zhou D, Yang R.** 2011. Phenotypic and transcriptional analysis of the osmotic regulator OmpR in Yersinia pestis. BMC Microbiol. **11**:39. doi:10.1186/1471-2180-11-39.
42. **Vidal O, Longin R, Prigent-Combaret C, Dorel C, Hooreman M, Lejeune P.** 1998. Isolation of an Escherichia coli K-12 mutant strain able to form biofilms on inert surfaces: involvement of a new ompR allele that increases curli expression. J. Bacteriol. **180**:2442–2449.
43. **Guisbert E, Yura T, Rhodius VA, Gross CA.** 2008. Convergence of molecular, modeling, and systems approaches for an understanding of the Escherichia coli heat shock response. Microbiol. Mol. Biol. Rev. **72**:545–554.
44. **Petranovic D, Michelsen O, Zahradka K, Silva C, Petranovic M, Jensen PR, Mijakovic I.** 2007. Bacillus subtilis strain deficient for the protein-tyrosine kinase PtkA exhibits impaired DNA replication. Mol. Microbiol. **63**:1797–1805.
45. **Fazli M, O'Connell A, Nilsson M, Niehaus K, Dow JM, Givskov M, Ryan RP, Tolker-Nielsen T.** 2011. The CRP/FNR family protein Bcam1349 is a c-di-GMP effector that regulates biofilm formation in the respiratory pathogen Burkholderia cenocepacia. Mol. Microbiol. **82**:327–341.
46. **Lee HS, Gu F, Ching SM, Lam Y, Chua KL.** 2010. CdpA is a Burkholderia pseudomallei cyclic di-GMP phosphodiesterase involved in autoaggregation, flagellum synthesis, motility, biofilm formation, cell invasion, and cytotoxicity. Infect. Immun. **78**:1832–1840.
47. **Kiley TB, Stanley-Wall NR.** 2010. Post-translational control of Bacillus subtilis biofilm formation mediated by tyrosine phosphorylation. Mol. Microbiol. **78**:947–963.
48. **Jers C, Soufi B, Grangeasse C, Deutscher J, Mijakovic I.** 2008. Phosphoproteomics in bacteria: towards a systemic understanding of bacterial phosphorylation networks. Expert Rev. Proteomics **5**:619–627.
49. **Ensgraber M, Loos M.** 1992. A 66-kilodalton heat shock protein of Salmonella typhimurium is responsible for binding of the bacterium to intestinal mucus. Infect. Immun. **60**:3072–3078.
50. **Hennequin C, Porcheray F, Waligora-Dupriet A, Collignon A, Barc M, Bourlioux P, Karjalainen T.** 2001. GroEL (Hsp60) of Clostridium difficile is involved in cell adherence. Microbiology **147**:87–96.
51. **Bullock WC, Fernandz JM, Short JM.** 1987. XL1-Blue: a high efficiency plasmid transforming recA Escherichia coli strain with beta-galactosidase selection. Biotechniques **5**:376–379.
52. **Figurski DH, Helinski DR.** 1979. Replication of an origin-containing derivative of plasmid RK2 dependent on a plasmid function provided in trans. Proc. Natl. Acad. Sci. U. S. A. **76**:1648–1652.
53. **Sokol PA, Darling P, Woods DE, Mahenthiralingam E, Kooi C.** 1999. Role of ornibactin biosynthesis in the virulence of Burkholderia cepacia: characterization of pvdA, the gene encoding L-ornithine N(5)-oxygenase. Infect. Immun. **67**:4443–4455.
54. **Keith KE, Valvano MA.** 2007. Characterization of SodC, a periplasmic superoxide dismutase from Burkholderia cenocepacia. Infect. Immun. **75**:2451–2460.
55. **Vergunst AC, Meijer AH, Renshaw SA, O'Callaghan D.** 2010. Burkholderia cenocepacia creates an intramacrophage replication niche in zebrafish embryos, followed by bacterial dissemination and establishment of systemic infection. Infect. Immun. **78**:1495–1508.